Precision measurement of the B_c^+ meson mass

The LHCb collaboration

E-mail: yanting.fan@cern.ch

ABSTRACT: A precision measurement of the B_c^+ meson mass is performed using proton-proton collision data collected with the LHCb experiment at centre-of-mass energies of $7, 8$ and $13 \, \mathrm{TeV}$, corresponding to a total integrated luminosity of 9.0 fb^{-1}. The B_c^+ mesons are reconstructed via the decays $B_c^+ \to J/\psi \, \pi^+$, $B_c^+ \to J/\psi \, \pi^+ \pi^- \pi^+$, $B_c^+ \to J/\psi \, p\bar{p}\pi^+$, $B_c^+ \to J/\psi \, D_s^+$, $B_c^+ \to J/\psi \, D^0 K^+$ and $B_c^+ \to B_s^0 \pi^+$. Combining the results of the individual decay channels, the B_c^+ mass is measured to be $6274.47 \pm 0.27 \, \text{(stat)} \pm 0.17 \, \text{(syst)} \, \mathrm{MeV}/c^2$. This is the most precise measurement of the B_c^+ mass to date. The difference between the B_c^+ and B_s^0 meson masses is measured to be $907.75 \pm 0.37 \, \text{(stat)} \pm 0.27 \, \text{(syst)} \, \mathrm{MeV}/c^2$.

https://doi.org/10.1007/JHEP07(2020)123

Contents

1 Introduction

The B_c meson family is unique in the Standard Model as its states contain two different heavy-flavour quarks, a $\bar{b}$ and a c quark. Quantum Chromodynamics (QCD) predicts that the $\bar{b}$ and c quarks are tightly bound in a compact system, with a rich spectroscopy of excited states. Studies of the B_c mass spectrum can reveal information on heavy-quark dynamics and improve our understanding of the strong interaction. Due to the presence of two heavy-flavour quarks the mass spectrum of the B_c states can be predicted with much better precision than many other hadronic systems. The mass spectrum of the B_c family has been calculated with nonrelativistic quark potential models [1–8], nonperturbative phenomenological models [9, 10], perturbative QCD [11, 12], relativistic quark models [13–17], and lattice QCD [18–23]. The ground state of the B_c meson family, denoted hereafter as B_c^+, decays only through the weak interaction, with a relatively long lifetime. The most accurate prediction of the B_c^+ mass, $M(B_c^+) = 6278 \pm 6 \pm 4 \,\text{MeV}/c^2$ [22], is obtained with unquenched lattice QCD.

In 1998 the CDF collaboration discovered the B_c^+ meson via its semileptonic decay modes and measured its mass to be $6400 \pm 390 \pm 130 \,\text{MeV}/c^2$ [24]. At the LHCb experiment, considerable progress has been made on measurements of the B_c^+ production [26–30], spectroscopy [26, 31–34], lifetime [35, 36], and new decay modes [30, 33, 37–45]. The world average of the B_c^+ mass has an uncertainty of $0.8 \,\text{MeV}/c^2$ [46]. This is the dominant systematic uncertainty in the recent $B_c(2S)^{(*)+}$ mass measurements [34, 47].

This paper presents a precision measurement of the B_c^+ mass using the decay modes $B_c^+ \to J/\psi \pi^+$, $B_c^+ \to J/\psi \pi^+ \pi^- \pi^+$, $B_c^+ \to J/\psi p\bar{p}\pi^+$, $B_c^+ \to J/\psi D_s^+$, $B_c^+ \to J/\psi D^0 K^+$ and

$B_c^+ \to B_s^0 \pi^+$.[1] The first two decays are chosen for their large signal yield, while the others have a low energy release. As the B_s^0 mass is known with limited precision, the difference between the B_c^+ and B_s^0 masses, $\Delta M = M(B_c^+) - M(B_s^0)$, is also measured, such that improvements in the B_s^+ mass measurement allow for a more precise B_c^+ mass determination. The data sample corresponds to an integrated luminosity of $9.0\,\mathrm{fb}^{-1}$, collected with the LHCb experiment in pp collisions at centre-of-mass energies of $7, 8$ and $13\,\mathrm{TeV}$. The integrated luminosity used in this analysis is at least three times the one used in previous LHCb measurements [26, 31–33] and the results of this paper supersede those earlier B_c^+ mass measurements.

2 Detector and simulation

This LHCb detector [48, 49] is a single-arm forward spectrometer covering the pseudorapidity range $2 < \eta < 5$, designed for the study of particles containing b or c quarks. The detector includes a high-precision tracking system consisting of a silicon-strip vertex detector surrounding the pp interaction region [50], a large-area silicon-strip detector located upstream of a dipole magnet with a bending power of about $4\,\mathrm{Tm}$, and three stations of silicon-strip detectors and straw drift tubes [51, 52] placed downstream of the magnet. The tracking system provides a measurement of the momentum, p, of charged particles with a relative uncertainty that varies from 0.5% at low momentum to 1.0% at $200\,\mathrm{GeV}/c$. The momentum scale is calibrated using samples of $B^+ \to J/\psi\,K^+$ and $J/\psi \to \mu^+\mu^-$ decays collected concurrently with the data sample used for this analysis [53, 54]. The relative accuracy of this procedure is determined to be 3×10^{-4} using samples of other fully reconstructed B, Υ and K_S^0-meson decays. The minimum distance of a track to a primary vertex (PV), the impact parameter (IP), is measured with a resolution of $(15 + 29/p_T)\,\mu\mathrm{m}$, where p_T is the component of the momentum transverse to the beam, in GeV/c. Different types of charged hadrons are distinguished using information from two ring-imaging Cherenkov detectors [55]. Photons, electrons and hadrons are identified by a calorimeter system consisting of a scintillating-pad and preshower detectors, an electromagnetic and a hadronic calorimeter. Muons are identified by a system composed of alternating layers of iron and multiwire proportional chambers [56]. The online event selection is performed by a trigger [57], which consists of a hardware stage, based on information from the calorimeter and muon systems, followed by a software stage, which performs a full event reconstruction.

Simulated samples are used to model the effects of the detector acceptance, optimise signal selection and validate the analysis technique. In simulation, pp collisions are generated using PYTHIA 8 [58] with an LHCb specific configuration [59]. The production of B_c^+ mesons is simulated using the dedicated generator BCVEGPY [60]. Decays of hadrons are described by EVTGEN [61], in which final-state radiation is generated using PHOTOS 3 [62]. The interaction of the generated particles with the detector and its response are implemented using the GEANT4 toolkit [63] as described in ref. [65].

---

[1] The inclusion of charge-conjugate modes is implied throughout this paper.

3 Event selection

The B_c^+ candidates are reconstructed in the following decay modes: $B_c^+ \to J/\psi\,\pi^+$, $B_c^+ \to J/\psi\,\pi^+\pi^-\pi^+$, $B_c^+ \to J/\psi\,p\bar{p}\pi^+$, $B_c^+ \to J/\psi\,D_s^+$, $B_c^+ \to J/\psi\,D^0K^+$ and $B_c^+ \to B_s^0\pi^+$. A pair of oppositely charged muons form J/ψ candidates. The D_s^+ candidates are reconstructed via the $D_s^+ \to K^+K^-\pi^+$ and $D_s^+ \to \pi^+\pi^-\pi^+$ decays, while the D^0 is reconstructed using the $D^0 \to K^-\pi^+$ decay. The B_s^0 candidates are reconstructed in the decay modes $B_s^0 \to J/\psi(\to \mu^+\mu^-)\phi(\to K^+K^-)$ and $B_s^0 \to D_s^-(\to K^+K^-\pi^-)\pi^+$, and a multivariate classifier as used in ref. [27] is employed to separate signal from combinatorial background. Then the B_s^0 candidates are combined with an additional pion to reconstruct B_c^+ candidates. All of the intermediate-state particles are required to have an invariant mass within three times the expected mass resolution around their known masses [46]. Muons, kaons, pions and protons are required to have good track-fit quality and high transverse momentum. The J/ψ and B_c^+ candidates are required to have a good-quality vertex fit.

A boosted decision tree [66–68] implemented within the TMVA [69] package optimises separation of the signal from combinatorial background for each decay mode. The classifiers are trained with simulated signal samples and a background proxy obtained from the upper mass sideband of the data, in the range $[6.6, 7.0]\,\mathrm{GeV}/c^2$. Kinematic variables that generically separate b-hadron decays from background are used in the training of the classifiers. The variables include the decay time, transverse momenta, vertex-fit quality of the B_c^+ candidate, as well as variables related to the fact that the B_c^+ meson is produced at the PV. The requirement on the classifiers is determined by maximising the signal significance $S/\sqrt{S+B}$, where S is the expected signal yield estimated using simulation, and B is the expected background yield evaluated in the upper sideband in data and extrapolated to the signal region.

4 Mass measurement

The B_c^+ meson mass is determined in each decay mode by performing an unbinned maximum likelihood fit to the invariant mass distributions of the B_c^+ candidates. The signal is described by a double-sided Crystal Ball (DSCB) function [70], while the background is described by an exponential function. The DSCB function comprises a Gaussian core with power-law tails to account for radiative effects. Parameters describing the radiative tails are determined from simulation.

The invariant mass of the B_c^+ candidates is calculated from a kinematic fit [71], in which the B_c^+ candidate is assumed to originate from its PV and the intermediate-state masses are constrained to their known values [46]. The PV of the B_c^+ candidate is that with respect to which it has the smallest χ_{IP}^2. The χ_{IP}^2 is defined as the difference in χ^2 of the PV fit with and without the particle in question. For $B_c^+ \to B_s^0\pi^+$ decays, the B_s^0 mass is constrained to the value of $5366.89 \pm 0.21\,\mathrm{MeV}/c^2$, which is an average of the measurements of the B_s^0 mass performed by the LHCb collaboration [72–75].

Decay mode	Yield	Fitted mass [MeV/c^2]	Corrected mass [MeV/c^2]	Resolution [MeV/c^2]
$J/\psi\,\pi^+$	25181 ± 217	6273.71 ± 0.12	6273.78 ± 0.12	13.49 ± 0.11
$J/\psi\,\pi^+\pi^-\pi^+$	9497 ± 142	6274.26 ± 0.18	6274.38 ± 0.18	11.13 ± 0.18
$J/\psi\,p\bar{p}\pi^+$	273 ± 29	6274.66 ± 0.73	6274.61 ± 0.73	6.34 ± 0.76
$J/\psi\,D_s^+(K^+K^-\pi^+)$	1135 ± 49	6274.09 ± 0.27	6274.11 ± 0.27	5.93 ± 0.30
$J/\psi\,D_s^+(\pi^+\pi^-\pi^+)$	202 ± 20	6274.57 ± 0.71	6274.29 ± 0.71	6.63 ± 0.67
$J/\psi\,D^0(K^-\pi^+)K^+$	175 ± 21	6273.97 ± 0.53	6274.08 ± 0.53	3.87 ± 0.57
$B_s^0(D_s^-\pi^+)\pi^+$	316 ± 27	6274.36 ± 0.44	6274.08 ± 0.44	4.67 ± 0.48
$B_s^0(J/\psi\,\phi)\pi^+$	299 ± 37	6275.87 ± 0.66	6275.46 ± 0.66	5.32 ± 0.74

Table 1. Signal yields, mass values and mass resolutions as obtained from fits shown in figure 1, together with the mass corrected for the effects of final-state radiation and selection as described in the text. The uncertainties are statistical only.

The difference between the B_c^+ and B_s^0 meson masses, $\Delta m = m(B_c^+) - m(B_s^0)$, is determined in the $B_c^+ \to B_s^0\pi^+$ decay mode, where $m(B_c^+)$ and $m(B_s^0)$ are the reconstructed masses of B_c^+ and B_s^0 candidates. The mass difference Δm is calculated with a kinematic fit [71], in which the B_c^+ candidate is assumed to originate from the PV with the smallest χ_{IP}^2 and the masses of the intermediate particles are constrained to their known values [46]. The fitting procedure for the mass difference is the same as for the mass fit.

Figure 1 shows the invariant mass distributions and fit results for all B_c^+ decay modes. Figure 2 shows the distributions of Δm and fit results for the $B_c^+ \to B_s^0(D_s^-\pi^+)\pi^+$ and $B_c^+ \to B_s^0(J/\psi\,\phi)\pi^+$ decay modes. The lower limit of the mass window is chosen to exclude the partially reconstructed background while keeping sufficient left mass sideband. The signal yields, mass and resolution values as determined from fits to the individual mass distributions are given in table 1. For the $B_c^+ \to B_s^0\pi^+$ decays, the results of the fits to the Δm distribution are reported in table 2.

The reconstructed invariant-mass distribution is distorted due to the missing energy from unreconstructed photons (bremsstrahlung) emitted by final-state particles. The resulting bias in the extracted B_c^+ mass is studied with simulated samples for each decay channel, and is used to correct the mass obtained from the fit. Multiple scattering in detector material can decrease the observed opening angles among the B_c^+ decay products, affecting the reconstructed B_c^+ mass and decay length and thereby the selection efficiency. Such effect distorts the mass distribution after the event selection. The corresponding bias of the B_c^+ mass measurement was studied with charmed hadrons ($D^+, D^0, D_s^+, \Lambda_c^+$), and was found to be well reproduced by simulation [76]. A bias associated with the selection from simulated samples is assigned as a corresponding correction. The measured masses (M) and mass difference (ΔM) are corrected for this bias (from -0.46 to $0.27\,\mathrm{MeV}/c^2$) due to final-state radiation and the selection, and summarised in table 1 and 2.
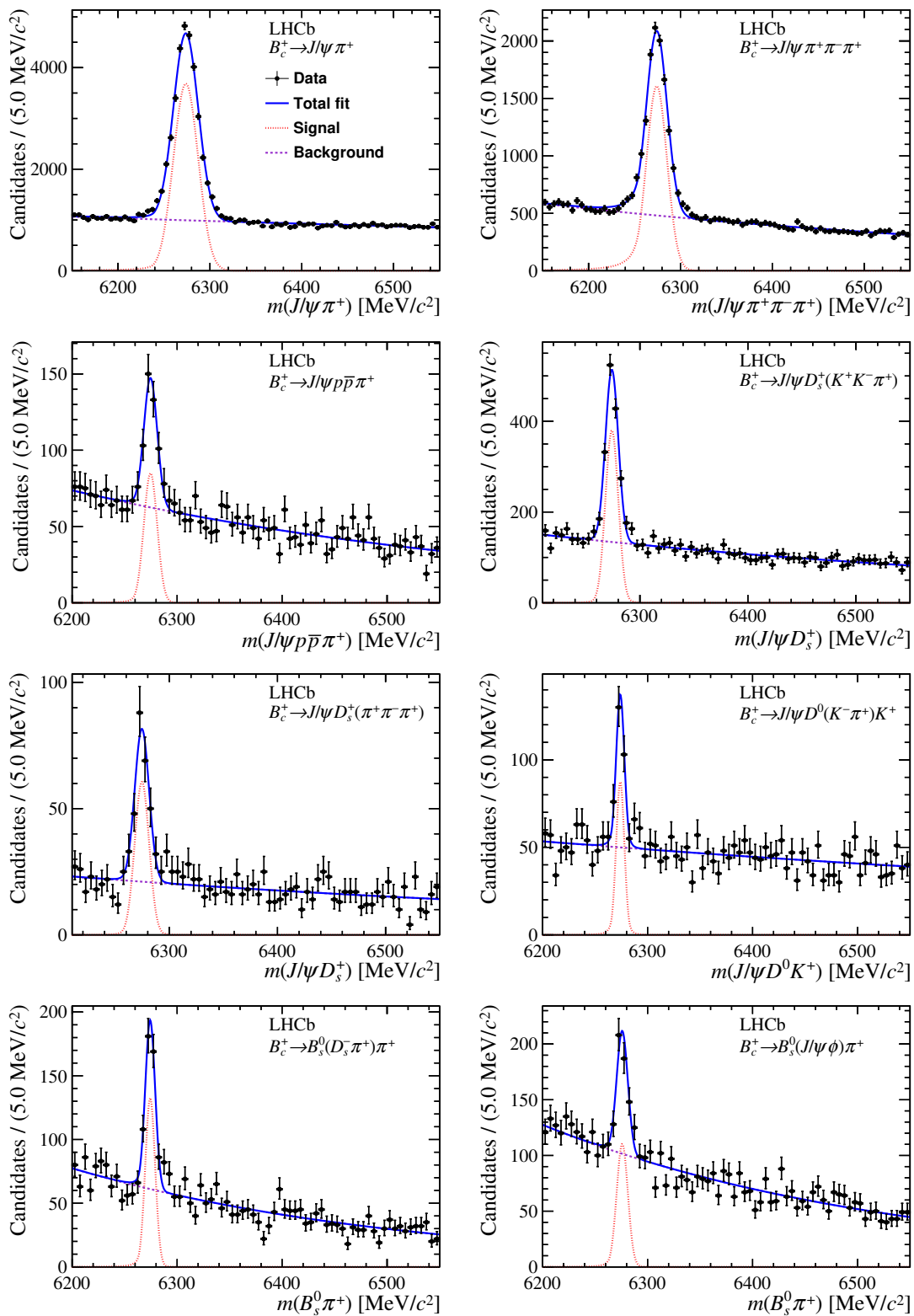
Figure 1. Distributions of invariant-mass m for B_c^+ candidates selected in the studied decay channels, where data are shown as the points with error bars; the total fits are shown as solid blue curves; the signal component are red dotted curves; the background components purple dotted curves.
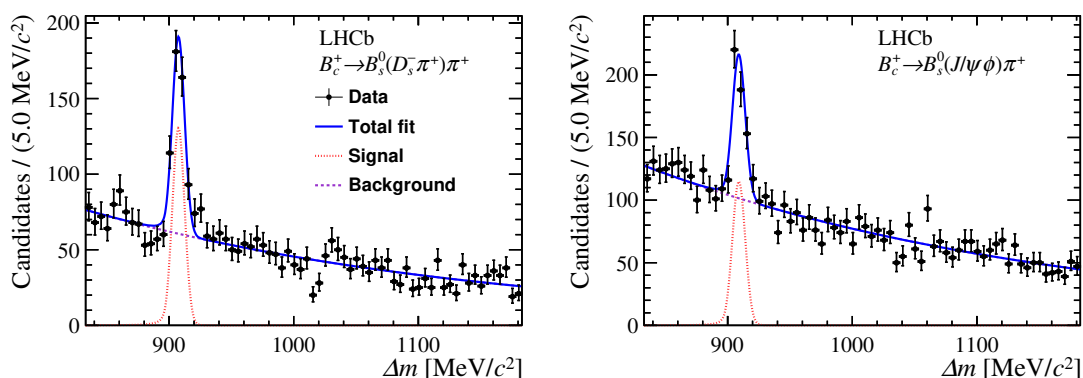
Figure 2. Distributions of mass difference Δm for the $B_c^+ \rightarrow B_s^0(D_s^-\pi^+)\pi^+$ and $B_c^+ \rightarrow B_s^0(J/\psi\,\phi)\pi^+$ decay modes, where data are shown as the points with error bars; the total fits are shown as solid blue curves; the signal component are red dotted curves; the background components purple dotted curves.

Decay mode	Yield	Fitted ΔM [MeV/c^2]	Corrected ΔM [MeV/c^2]	Resolution [MeV/c^2]
$B_s^0(D_s^-\pi^+)\pi^+$	325 ± 27	907.51 ± 0.46	907.24 ± 0.46	4.88 ± 0.47
$B_s^0(J/\psi\,\phi)\pi^+$	300 ± 32	908.98 ± 0.61	908.59 ± 0.61	5.12 ± 0.62

Table 2. Signal yields, mass difference (ΔM) and resolution as obtained from fits shown in figure 2, together with the values corrected for the effects of final-state radiation and selection as described in the text. The uncertainties are statistical only.

5 Systematic uncertainties

To evaluate systematic uncertainties, the complete analysis is repeated varying assumed parameters, models and selection requirements. The observed differences in the B_c^+ mass central values between the nominal result and the alternative estimates are considered as one standard-deviation uncertainties.

The systematic uncertainty of the B_c^+ mass comprises uncertainties on the momentum-scale calibration, energy loss corrections, signal and background models, the mass of the intermediate states and the uncertainty on the bias caused by the final-state radiation and selection.

The dominant source of systematic uncertainty arises due to the limited precision of the momentum-scale calibration. For each decay, this uncertainty is propagated to the B_c^+ mass according to the energy release, which is the difference between the value of the B_c^+ mass and the sum of the masses of its intermediate states. The amount of material traversed in the tracking system by a particle is known to 10% accuracy, which leads to an uncertainty on the estimated energy loss. This translates into a measured mass uncertainty of $0.03 \, \mathrm{MeV}/c^2$ for $D^0 \rightarrow K^+K^-\pi^+\pi^-$ decays [54]. The uncertainties on the B_c^+ mass are scaled from that of the D^0 decay by the number of final-state particles. The uncertainties due to the limited size of simulated samples are taken as systematic uncertainties from the

Decay mode	Momentum scale calibration	Energy loss correction	Signal model	Background model	Intermediate states	Selection	Total
$J/\psi\,\pi^+$	0.91	0.02	0.10	0.01	<0.01	0.01	0.92
$J/\psi\,\pi^+\pi^-\pi^+$	0.83	0.04	0.10	0.02	<0.01	0.05	0.84
$J/\psi\,p\bar{p}\pi^+$	0.35	0.04	0.10	0.01	<0.01	0.06	0.37
$J/\psi\,D_s^+(K^+K^-\pi^+)$	0.36	0.04	0.10	0.02	0.07	0.02	0.38
$J/\psi\,D_s^+(\pi^+\pi^-\pi^+)$	0.36	0.04	0.10	0.02	0.07	0.03	0.38
$J/\psi\,D^0(K^-\pi^+)K^+$	0.25	0.04	0.10	0.01	0.05	0.02	0.28
$B_s^0(D_s^-\pi^+)\pi^+$	0.23	0.04	0.10	<0.01	0.21	0.12	0.43
$B_s^0(J/\psi\,\phi)\pi^+$	0.23	0.04	0.10	0.01	0.21	0.02	0.41

Table 3. Summary of systematic uncertainties (in MeV/c^2) on the B_c^+ mass.

Decay mode	Momentum scale calibration	Energy loss	Signal model	Background model	Intermediate states	Selection	Total
$B_s^0(D_s^-\pi^+)\pi^+$	0.23	0.04	0.10	0.01	<0.01	0.13	0.29
$B_s^0(J/\psi\,\phi)\pi^+$	0.23	0.04	0.10	<0.01	<0.01	0.02	0.25

Table 4. Summary of systematic uncertainties on the mass difference ΔM (in MeV/c^2) for the $B_s^0(D_s^-\pi^+)\pi^+$ and $B_s^0(J/\psi\,\phi)\pi^+$ decays.

selection-induced bias on the B_c^+ masses. The uncertainty on the masses of the intermediate states D_s^+, D^0, B_s^0 are propagated to the B_c^+ mass measurement.

The uncertainty related to the signal shape is estimated by using alternative signal models, including the sum of two Gaussian functions, a Hypatia function [77], the sum of a DSCB and a Gaussian function, and the sum of two DSCB functions. The differences of the fitted mass with final-state radiation corrections between the nominal and the alternative models are found to be smaller than $0.1\,\mathrm{MeV}/c^2$, which is taken as the corresponding systematic uncertainty. The uncertainty related to the background description is evaluated by using a first-order Chebyshev function instead of an exponential function.

The non-resonant contribution, for example the contribution of $B_c^+ \to J/\psi\,\pi^+\pi^-\pi^+$ decays to the $B_c^+ \to J/\psi\,D_s^+(\pi^+\pi^-\pi^+)$ candidates, is found to be highly suppressed and have negligible effects on the mass measurement. The systematic uncertainties considered for the B_c^+ mass and mass difference measurements are summarised in table 3 and 4, respectively.

6 Combination of the measurements

The combination of the B_c^+ mass measurements is performed using the Best Linear Unbiased Estimate (BLUE) method [78–80]. In the combination, uncertainties arising from the momentum-scale calibration, energy loss corrections, and signal model are assumed to be 100% correlated, while all other sources of systematic uncertainty are assumed to be uncor-
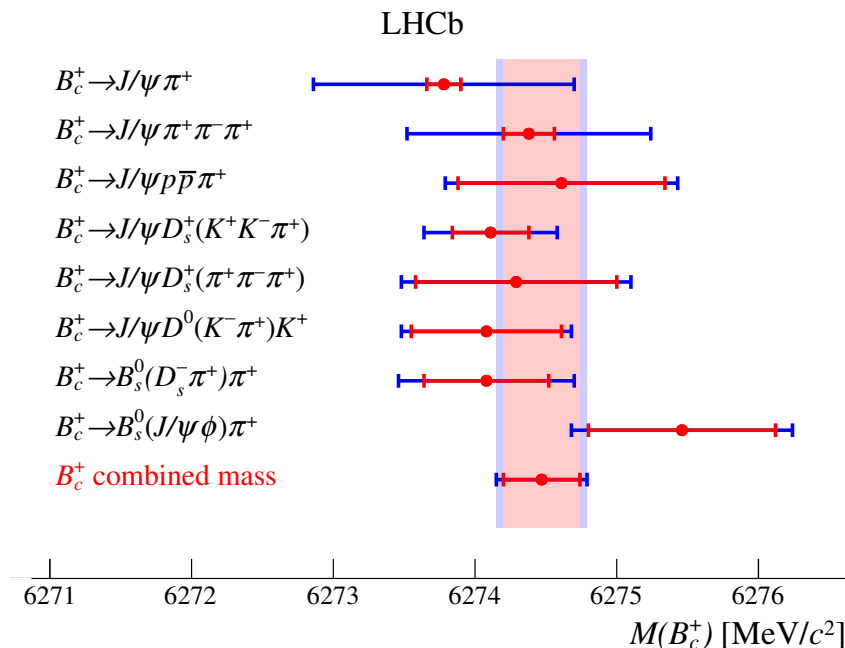
Figure 3. Individual B_c^+ mass measurements and their combination. The red (inner) cross-bars show the statistical uncertainties, and the blue (outer) cross-bars show the total uncertainties.

related. The uncertainty on the momentum-scale calibration of the B_s^0 mass ($0.14\,\mathrm{MeV}/c^2$) is assumed to be 100% correlated with that of the B_c^+ mass.

The individual mass measurements and the resulting combination are shown in figure 3. The individual measurements are consistent with each other. The breakdown of the combined systematic uncertainty is given in table 5. The weights of individual measurements returned by the BLUE method are listed in table 6. The weights are computed including all uncertainties. The measurement contributing most to the combination is obtained from the $B_c^+ \to J/\psi\, D_s^+(K^+K^-\pi^+)$ decay. The negative weight for the $B_c^+ \to J/\psi\,\pi^+$ channel arises from the 100% correlation between the systematic uncertainties due to the momentum-scale calibration. This results in a larger statistical and smaller systematic uncertainty relative to an uncorrelated average.

The combination for the mass difference ΔM is shown in figure 4. The breakdown of the combined systematic uncertainty is given in table 5 and the weights of decay modes in the combination are listed in table 6. The combined B_c^+ mass is determined to be $M(B_c^+) = 6274.47 \pm 0.27\,(\text{stat}) \pm 0.17\,(\text{syst})\,\mathrm{MeV}/c^2$, while the mass difference between the B_c^+ and B_s^0 mesons, ΔM, is determined to be $\Delta M = 907.75 \pm 0.37\,(\text{stat}) \pm 0.27\,(\text{syst})\,\mathrm{MeV}/c^2$.

7 Summary

In summary, a precise measurement of the B_c^+ mass is performed using data samples collected in pp collisions with the LHCb experiment at centre-of-mass energies of $\sqrt{s} = 7$, 8 and 13 TeV, corresponding to an integrated luminosity of $9\,\mathrm{fb}^{-1}$. The B_c^+ candidates

Source	Mass	Mass difference
Momentum-scale calibration	0.11	0.23
Energy loss	0.05	0.04
Signal line shape	0.10	0.10
Background line shape	0.01	0.01
Mass of intermediate state	0.06	<0.01
Selection bias correction	0.03	0.08
Total	0.17	0.27

Table 5. Breakdown of systematic uncertainties (in MeV/c^2) in the combination of the B_c^+ mass and the mass difference ΔM. The total uncertainty is the sum in quadrature of the uncertainty of different sources.

Decay mode	Mass	Mass difference
$J/\psi\,\pi^+$	-0.446	—
$J/\psi\,\pi^+\pi^-\pi^+$	0.032	—
$J/\psi\,p\bar{p}\pi^+$	0.098	—
$J/\psi\,D_s^+(K^+K^-\pi^+)$	0.659	—
$J/\psi\,D_s^+(\pi^+\pi^-\pi^+)$	0.101	—
$J/\psi\,D^0(K^-\pi^+)K^+$	0.224	—
$B_s^0(D_s^-\pi^+)\pi^+$	0.220	0.620
$B_s^0(J/\psi\,\phi)\pi^+$	0.111	0.380

Table 6. Weights of the decay modes in the combination of the B_c^+ mass and the mass difference ΔM.
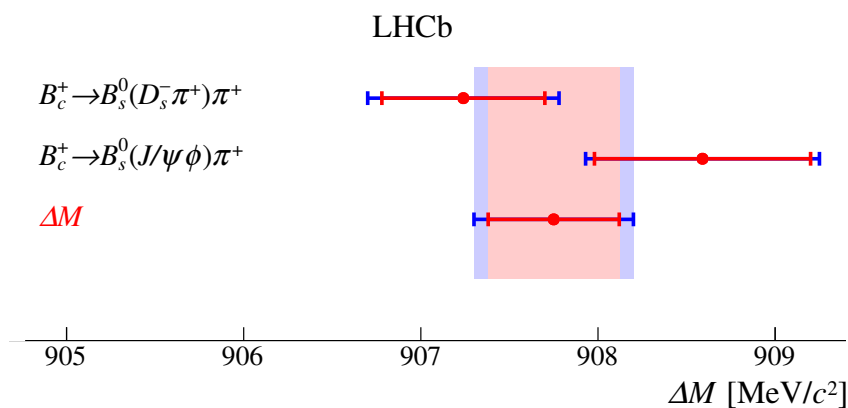

Figure 4. Individual mass difference measurements and their combination. The red (inner) cross-bars show the statistical uncertainties, and the blue (outer) cross-bars show the total uncertainties on the measurement.

are reconstructed via the decays $B_c^+ \to J/\psi\,\pi^+$, $B_c^+ \to J/\psi\,\pi^+\pi^-\pi^+$, $B_c^+ \to J/\psi\,p\bar{p}\pi^+$, $B_c^+ \to J/\psi\,D_s^+(K^+K^-\pi^+)$, $B_c^+ \to J/\psi\,D_s^+(\pi^+\pi^-\pi^+)$, $B_c^+ \to J/\psi\,D^0(K^-\pi^+)K^+$, $B_c^+ \to B_s^0(D_s^-\pi^+)\pi^+$ and $B_c^+ \to B_s^0(J/\psi\,\phi)\pi^+$. The B_c^+ mass is determined to be

$$6274.47 \pm 0.27\,(\text{stat}) \pm 0.17\,(\text{syst})\,\text{MeV}/c^2.$$

This result is consistent with theoretical predictions from perturbative and lattice QCD. The mass difference between the B_c^+ and B_s^0 mesons, ΔM, is determined to be

$$907.75 \pm 0.37\,(\text{stat}) \pm 0.27\,(\text{syst})\,\text{MeV}/c^2.$$

These results are the most accurate measurements of the B_c^+ mass to date. The precision compared to the world average [46] is improved by a factor of 2.

Acknowledgments

References

[1] S.S. Gershtein et al., *Production cross-section and spectroscopy of B_c mesons*, *Sov. J. Nucl. Phys.* **48** (1988) 327 [ɪɴSPIRE].

[2] Y.-Q. Chen and Y.-P. Kuang, *Improved QCD motivated heavy quark potentials with explicit Lambda(ms) dependence*, *Phys. Rev. D* **46** (1992) 1165 [*Erratum ibid.* **47** (1993) 350] [ɪɴSPIRE].

[3] E.J. Eichten and C. Quigg, *Mesons with beauty and charm: Spectroscopy*, *Phys. Rev. D* **49** (1994) 5845 [hep-ph/9402210] [INSPIRE].

[4] S.S. Gershtein, V.V. Kiselev, A.K. Likhoded and A.V. Tkabladze, B_c *spectroscopy*, *Phys. Rev. D* **51** (1995) 3613 [hep-ph/9406339] [INSPIRE].

[5] S.N. Gupta and J.M. Johnson, B_c *spectroscopy in a quantum chromodynamic potential model*, *Phys. Rev. D* **53** (1996) 312 [hep-ph/9511267] [INSPIRE].

[6] L.P. Fulcher, *Phenomenological predictions of the properties of the B_c system*, *Phys. Rev. D* **60** (1999) 074006 [hep-ph/9806444] [INSPIRE].

[7] N. Devlani, V. Kher and A.K. Rai, *Masses and electromagnetic transitions of the B_c mesons*, *Eur. Phys. J. A* **50** (2014) 154 [INSPIRE].

[8] N.R. Soni, B.R. Joshi, R.P. Shah, H.R. Chauhan and J.N. Pandya, $Q\bar{Q}$ $(Q \in \{b, c\})$ *spectroscopy using the Cornell potential*, *Eur. Phys. J. C* **78** (2018) 592 [arXiv:1707.07144] [INSPIRE].

[9] K.-W. Wei and X.-H. Guo, *Mass spectra of doubly heavy mesons in Regge phenomenology*, *Phys. Rev. D* **81** (2010) 076005 [INSPIRE].

[10] M. Chen, L. Chang and Y.-x. Liu, B_c *meson spectrum via Dyson-Schwinger equation and Bethe-Salpeter equation approach*, *Phys. Rev. D* **101** (2020) 056002 [arXiv:2001.00161] [INSPIRE].

[11] N. Brambilla and A. Vairo, *The B_c mass up to order α_s^4*, *Phys. Rev. D* **62** (2000) 094019 [hep-ph/0002075] [INSPIRE].

[12] Z.-J. Xiao and X. Liu, *The two-body hadronic decays of B_c meson in the perturbative QCD approach: A short review*, *Chin. Sci. Bull.* **59** (2014) 3748 [arXiv:1401.0151] [INSPIRE].

[13] D. Ebert, R.N. Faustov and V.O. Galkin, *Properties of heavy quarkonia and B_c mesons in the relativistic quark model*, *Phys. Rev. D* **67** (2003) 014027 [hep-ph/0210381] [INSPIRE].

[14] S. Godfrey, *Spectroscopy of B_c mesons in the relativized quark model*, *Phys. Rev. D* **70** (2004) 054017 [hep-ph/0406228] [INSPIRE].

[15] D. Ebert, R.N. Faustov and V.O. Galkin, *Spectroscopy and Regge trajectories of heavy quarkonia and B_c mesons*, *Eur. Phys. J. C* **71** (2011) 1825 [arXiv:1111.0454] [INSPIRE].

[16] C.S. Fischer, S. Kubrak and R. Williams, *Spectra of heavy mesons in the Bethe-Salpeter approach*, *Eur. Phys. J. A* **51** (2015) 10 [arXiv:1409.5076] [INSPIRE].

[17] A.P. Monteiro, M. Bhat and K.B. Vijaya Kumar, $c\bar{b}$ *spectrum and decay properties with coupled channel effects*, *Phys. Rev. D* **95** (2017) 054016 [arXiv:1608.05782] [INSPIRE].

[18] C.T.H. Davies, K. Hornbostel, G.P. Lepage, A.J. Lidsey, J. Shigemitsu and J.H. Sloan, B_c *spectroscopy from lattice QCD*, *Phys. Lett. B* **382** (1996) 131 [hep-lat/9602020] [INSPIRE].

[19] UKQCD collaboration, *A nonperturbative calculation of the mass of the B_c*, *Phys. Lett. B* **453** (1999) 289 [hep-lat/9902025] [INSPIRE].

[20] HPQCD, FNAL LATTICE and UKQCD collaborations, *A precise determination of the B_c mass from dynamical lattice QCD*, *Nucl. Phys. Proc. Suppl.* **140** (2005) 440 [hep-lat/0409090] [INSPIRE].

[21] HPQCD, FERMILAB LATTICE and UKQCD collaborations, *Mass of the B_c meson in three-flavor lattice QCD*, *Phys. Rev. Lett.* **94** (2005) 172001 [hep-lat/0411027] [INSPIRE].

[22] TWQCD collaboration, B_s and B_c mesons in lattice QCD with exact chiral symmetry, PoS **LAT2006** (2007) 180 [`arXiv:0704.3495`] [INSPIRE].

[23] R.J. Dowdall, C.T.H. Davies, T.C. Hammant and R.R. Horgan, *Precise heavy-light meson masses and hyperfine splittings from lattice QCD including charm quarks in the sea*, Phys. Rev. D **86** (2012) 094510 [`arXiv:1207.5149`] [INSPIRE].

[24] CDF collaboration, *Observation of the B_c meson in $p\bar{p}$ collisions at $\sqrt{s} = 1.8$ TeV*, Phys. Rev. Lett. **81** (1998) 2432 [`hep-ex/9805034`] [INSPIRE].

[25] CDF collaboration, *Observation of B_c mesons in $p\bar{p}$ collisions at $\sqrt{s} = 1.8$ TeV*, Phys. Rev. D **58** (1998) 112004 [`hep-ex/9804014`] [INSPIRE].

[26] LHCb collaboration, *Measurements of B_c^+ production and mass with the $B_c^+ \to J/\psi\pi^+$ decay*, Phys. Rev. Lett. **109** (2012) 232001 [`arXiv:1209.5634`] [INSPIRE].

[27] LHCb collaboration, *Observation of the Decay $B_c^+ \to B_s^0\pi^+$*, Phys. Rev. Lett. **111** (2013) 181801 [`arXiv:1308.4544`] [INSPIRE].

[28] LHCb collaboration, *Measurement of the B_c^- meson production fraction and asymmetry in 7 and 13 TeV pp collisions*, Phys. Rev. D **100** (2019) 112006 [`arXiv:1910.13404`] [INSPIRE].

[29] LHCb collaboration, *Measurement of B_c^+ production in proton-proton collisions at $\sqrt{s} = 8$ TeV*, Phys. Rev. Lett. **114** (2015) 132001 [`arXiv:1411.2943`] [INSPIRE].

[30] LHCb collaboration, *Observation of $B_c^+ \to D^0K^+$ decays*, Phys. Rev. Lett. **118** (2017) 111803 [`arXiv:1701.01856`] [INSPIRE].

[31] LHCb collaboration, *Observation of $B_c^+ \to J/\psi D_s^+$ and $B_c^+ \to J/\psi D_s^{*+}$ decays*, Phys. Rev. D **87** (2013) 112012 [*Addendum ibid.* **89** (2014) 019901] [`arXiv:1304.4530`] [INSPIRE].

[32] LHCb collaboration, *First observation of a baryonic B_c^+ decay*, Phys. Rev. Lett. **113** (2014) 152003 [`arXiv:1408.0971`] [INSPIRE].

[33] LHCb collaboration, *Observation of $B_c^+ \to J/\psi D^{(*)}K^{(*)}$ decays*, Phys. Rev. D **95** (2017) 032005 [`arXiv:1612.07421`] [INSPIRE].

[34] LHCb collaboration, *Observation of an excited B_c^+ state*, Phys. Rev. Lett. **122** (2019) 232001 [`arXiv:1904.00081`] [INSPIRE].

[35] LHCb collaboration, *Measurement of the B_c^+ meson lifetime using $B_c^+ \to J/\psi\mu^+\nu_\mu X$ decays*, Eur. Phys. J. C **74** (2014) 2839 [`arXiv:1401.6932`] [INSPIRE].

[36] LHCb collaboration, *Measurement of the lifetime of the B_c^+ meson using the $B_c^+ \to J/\psi\pi^+$ decay mode*, Phys. Lett. B **742** (2015) 29 [`arXiv:1411.6899`] [INSPIRE].

[37] LHCb collaboration, *Observation of the decay $B_c^+ \to \psi(2S)\pi^+$*, Phys. Rev. D **87** (2013) 071103 [`arXiv:1303.1737`] [INSPIRE].

[38] LHCb collaboration, *First observation of the decay $B_c^+ \to J/\psi K^+$*, JHEP **09** (2013) 075 [`arXiv:1306.6723`] [INSPIRE].

[39] LHCb collaboration, *Observation of the decay $B_c \to J/\psi K^+K^-\pi^+$*, JHEP **11** (2013) 094 [`arXiv:1309.0587`] [INSPIRE].

[40] LHCb collaboration, *Measurement of the branching fraction ratio $\mathcal{B}(B_c^+ \to \psi(2S)\pi^+)/\mathcal{B}(B_c^+ \to J/\psi\pi^+)$*, Phys. Rev. D **92** (2015) 072007 [`arXiv:1507.03516`] [INSPIRE].

[41] LHCb collaboration, *Measurement of the ratio of branching fractions $\mathcal{B}(B_c^+ \to J/\psi K^+)/\mathcal{B}(B_c^+ \to J/\psi\pi^+)$*, JHEP **09** (2016) 153 [`arXiv:1607.06823`] [INSPIRE].

[42] LHCb collaboration, *Search for B_c^+ decays to the $p\bar{p}\pi^+$ final state*, *Phys. Lett. B* **759** (2016) 313 [arXiv:1603.07037] [INSPIRE].

[43] LHCb collaboration, *Study of B_c^+ decays to the $K^+K^-\pi^+$ final state and evidence for the decay $B_c^+ \to \chi_{c0}\pi^+$*, *Phys. Rev. D* **94** (2016) 091102 [arXiv:1607.06134] [INSPIRE].

[44] LHCb collaboration, *Measurement of the ratio of branching fractions $\mathcal{B}(B_c^+ \to J/\psi\tau^+\nu_\tau)/\mathcal{B}(B_c^+ \to J/\psi\mu^+\nu_\mu)$*, *Phys. Rev. Lett.* **120** (2018) 121801 [arXiv:1711.05623] [INSPIRE].

[45] LHCb collaboration, *Search for B_c^+ decays to two charm mesons*, *Nucl. Phys. B* **930** (2018) 563 [arXiv:1712.04702] [INSPIRE].

[46] PARTICLE DATA GROUP collaboration, *Review of Particle Physics*, *Phys. Rev. D* **98** (2018) 030001 [INSPIRE].

[47] CMS collaboration, *Observation of Two Excited B_c^+ States and Measurement of the $B_c^+(2S)$ Mass in pp Collisions at $\sqrt{s} = 13$ TeV*, *Phys. Rev. Lett.* **122** (2019) 132001 [arXiv:1902.00571] [INSPIRE].

[48] LHCb collaboration, *The LHCb Detector at the LHC*, 2008 *JINST* **3** S08005 [INSPIRE].

[49] LHCb collaboration, *LHCb Detector Performance*, *Int. J. Mod. Phys. A* **30** (2015) 1530022 [arXiv:1412.6352] [INSPIRE].

[50] R. Aaij et al., *Performance of the LHCb Vertex Locator*, 2014 *JINST* **9** P09007 [arXiv:1405.7808] [INSPIRE].

[51] LHCB OUTER TRACKER GROUP collaboration, *Performance of the LHCb Outer Tracker*, 2014 *JINST* **9** P01002 [arXiv:1311.3893] [INSPIRE].

[52] LHCB OUTER TRACKER GROUP collaboration, *Improved performance of the LHCb Outer Tracker in LHC Run 2*, 2017 *JINST* **12** P11016 [arXiv:1708.00819] [INSPIRE].

[53] LHCb collaboration, *Measurement of the Λ_b^0, Ξ_b^- and Ω_b^- baryon masses*, *Phys. Rev. Lett.* **110** (2013) 182001 [arXiv:1302.1072] [INSPIRE].

[54] LHCb collaboration, *Precision measurement of D meson mass differences*, *JHEP* **06** (2013) 065 [arXiv:1304.6865] [INSPIRE].

[55] LHCB RICH GROUP collaboration, *Performance of the LHCb RICH detector at the LHC*, *Eur. Phys. J. C* **73** (2013) 2431 [arXiv:1211.6759] [INSPIRE].

[56] A.A. Alves Jr. *Performance of the LHCb muon system*, 2013 *JINST* **8** P02022 [arXiv:1211.1346] [INSPIRE].

[57] R. Aaij et al., *The LHCb Trigger and its Performance in 2011*, 2013 *JINST* **8** P04022 [arXiv:1211.3055] [INSPIRE].

[58] T. Sjöstrand, S. Mrenna and P.Z. Skands, *A Brief Introduction to PYTHIA 8.1*, *Comput. Phys. Commun.* **178** (2008) 852 [arXiv:0710.3820] [INSPIRE].

[59] LHCb collaboration, *Handling of the generation of primary events in Gauss, the LHCb simulation framework*, *J. Phys. Conf. Ser.* **331** (2011) 032047 [INSPIRE].

[60] C.-H. Chang, J.-X. Wang and X.-G. Wu, *BCVEGPY2.0: A upgrade version of the generator BCVEGPY with an addendum about hadroproduction of the P-wave B_c states*, *Comput. Phys. Commun.* **174** (2006) 241 [hep-ph/0504017] [INSPIRE].

[61] D.J. Lange, *The EvtGen particle decay simulation package*, *Nucl. Instrum. Meth. A* **462** (2001) 152 [INSPIRE].

[62] P. Golonka and Z. Was, *PHOTOS Monte Carlo: A precision tool for QED corrections in Z and W decays*, *Eur. Phys. J. C* **45** (2006) 97 [hep-ph/0506026] [INSPIRE].

[63] GEANT4 collaboration, *Geant4 developments and applications*, *IEEE Trans. Nucl. Sci.* **53** (2006) 270.

[64] GEANT4 collaboration, *GEANT4 — a simulation toolkit*, *Nucl. Instrum. Meth. A* **506** (2003) 250 [INSPIRE].

[65] LHCb collaboration, *The LHCb simulation application, Gauss: Design, evolution and experience*, *J. Phys. Conf. Ser.* **331** (2011) 032023 [INSPIRE].

[66] L. Breiman, J. Friedman, R.A. Olshen and C.J. Stone, *Classification and regression trees*, Chapman and Hall/CRC, (1984).

[67] Y. Freund and R.E. Schapire, *A decision-theoretic generalization of on-line learning and an application to boosting*, *J. Comput. Syst. Sci.* **55** (1997) 119.

[68] J.H. Friedman, *Greedy function approximation: A gradient boosting machine*, *Ann. Statist.* **29** (2001) 1189.

[69] A. Hocker et al., *TMVA — Toolkit for Multivariate Data Analysis*, physics/0703039 [INSPIRE].

[70] T. Skwarnicki, *A study of the radiative cascade transitions between the Upsilon-prime and Upsilon resonances*, Ph.D. Thesis, Institute of Nuclear Physics, Krakow, (1986), DESY-F31-86-02 [INSPIRE].

[71] W.D. Hulsbergen, *Decay chain fitting with a Kalman filter*, *Nucl. Instrum. Meth. A* **552** (2005) 566 [physics/0503191] [INSPIRE].

[72] LHCb collaboration, *Observation of $B^0_{(s)} \to J/\psi p\overline{p}$ decays and precision measurements of the $B^0_{(s)}$ masses*, *Phys. Rev. Lett.* **122** (2019) 191804 [arXiv:1902.05588] [INSPIRE].

[73] LHCb collaboration, *Observation of the decay $\overline{B}^0_s \to \chi_{c2} K^+ K^-$ in the φ mass region*, *JHEP* **08** (2018) 191 [arXiv:1806.10576] [INSPIRE].

[74] LHCb collaboration, *Observation of the $B^0_s \to J/\psi\phi\phi$ decay*, *JHEP* **03** (2016) 040 [arXiv:1601.05284] [INSPIRE].

[75] LHCb collaboration, *Measurement of b-hadron masses*, *Phys. Lett. B* **708** (2012) 241 [arXiv:1112.4896] [INSPIRE].

[76] LHCb collaboration, *Observation of the doubly charmed baryon Ξ_{cc}^{++}*, *Phys. Rev. Lett.* **119** (2017) 112001 [arXiv:1707.01621] [INSPIRE].

[77] D. Martínez Santos and F. Dupertuis, *Mass distributions marginalized over per-event errors*, *Nucl. Instrum. Meth. A* **764** (2014) 150 [arXiv:1312.5000] [INSPIRE].

[78] L. Lyons, D. Gibaut and P. Clifford, *How to Combine Correlated Estimates of a Single Physical Quantity*, *Nucl. Instrum. Meth. A* **270** (1988) 110 [INSPIRE].

[79] A. Valassi, *Combining correlated measurements of several different physical quantities*, *Nucl. Instrum. Meth. A* **500** (2003) 391 [INSPIRE].

[80] R. Nisius, *BLUE: combining correlated estimates of physics observables within ROOT using the Best Linear Unbiased Estimate method*, arXiv:2001.10310 [INSPIRE].

The LHCb collaboration

R. Aaij[31], C. Abellán Beteta[49], T. Ackernley[59], B. Adeva[45], M. Adinolfi[53], H. Afsharnia[9],
C.A. Aidala[81], S. Aiola[25], Z. Ajaltouni[9], S. Akar[66], J. Albrecht[14], F. Alessio[47], M. Alexander[58],
A. Alfonso Albero[44], G. Alkhazov[37], P. Alvarez Cartelle[60], A.A. Alves Jr[45], S. Amato[2],
Y. Amhis[11], L. An[21], L. Anderlini[21], G. Andreassi[48], M. Andreotti[20], F. Archilli[16],
A. Artamonov[43], M. Artuso[67], K. Arzymatov[41], E. Aslanides[10], M. Atzeni[49], B. Audurier[11],
S. Bachmann[16], J.J. Back[55], S. Baker[60], V. Balagura[11,b], W. Baldini[20], J. Baptista Leite[1],
R.J. Barlow[61], S. Barsuk[11], W. Barter[60], M. Bartolini[23,47,h], F. Baryshnikov[78], J.M. Basels[13],
G. Bassi[28], V. Batozskaya[35], B. Batsukh[67], A. Battig[14], A. Bay[48], M. Becker[14], F. Bedeschi[28],
I. Bediaga[1], A. Beiter[67], V. Belavin[41], S. Belin[26], V. Bellee[48], K. Belous[43], I. Belyaev[38],
G. Bencivenni[22], E. Ben-Haim[12], S. Benson[31], A. Berezhnoy[39], R. Bernet[49], D. Berninghoff[16],
H.C. Bernstein[67], C. Bertella[47], E. Bertholet[12], A. Bertolin[27], C. Betancourt[49], F. Betti[19,e],
M.O. Bettler[54], Ia. Bezshyiko[49], S. Bhasin[53], J. Bhom[33], M.S. Bieker[14], S. Bifani[52], P. Billoir[12],
A. Bizzeti[21,t], M. Bjørn[62], M.P. Blago[47], T. Blake[55], F. Blanc[48], S. Blusk[67], D. Bobulska[58],
V. Bocci[30], O. Boente Garcia[45], T. Boettcher[63], A. Boldyrev[79], A. Bondar[42,w], N. Bondar[37,47],
S. Borghi[61], M. Borisyak[41], M. Borsato[16], J.T. Borsuk[33], T.J.V. Bowcock[59], A. Boyer[47],
C. Bozzi[20], M.J. Bradley[60], S. Braun[65], A. Brea Rodriguez[45], M. Brodski[47], J. Brodzicka[33],
A. Brossa Gonzalo[55], D. Brundu[26], E. Buchanan[53], A. Büchler-Germann[49], A. Buonaura[49],
C. Burr[47], A. Bursche[26], A. Butkevich[40], J.S. Butter[31], J. Buytaert[47], W. Byczynski[47],
S. Cadeddu[26], H. Cai[72], R. Calabrese[20,g], L. Calero Diaz[22], S. Cali[22], R. Calladine[52], M. Calvi[24,i],
M. Calvo Gomez[44,l], P. Camargo Magalhaes[53], A. Camboni[44,l], P. Campana[22],
D.H. Campora Perez[31], A.F. Campoverde Quezada[5], L. Capriotti[19,e], A. Carbone[19,e],
G. Carboni[29], R. Cardinale[23,h], A. Cardini[26], I. Carli[6], P. Carniti[24,i], K. Carvalho Akiba[31],
A. Casais Vidal[45], G. Casse[59], M. Cattaneo[47], G. Cavallero[47], S. Celani[48], R. Cenci[28,o],
J. Cerasoli[10], M.G. Chapman[53], M. Charles[12], Ph. Charpentier[47], G. Chatzikonstantinidis[52],
M. Chefdeville[8], V. Chekalina[41], C. Chen[3], S. Chen[26], A. Chernov[33], S.-G. Chitic[47],
V. Chobanova[45], S. Cholak[48], M. Chrzaszcz[33], A. Chubykin[37], V. Chulikov[37], P. Ciambrone[22],
M.F. Cicala[55], X. Cid Vidal[45], G. Ciezarek[47], F. Cindolo[19], P.E.L. Clarke[57], M. Clemencic[47],
H.V. Cliff[54], J. Closier[47], J.L. Cobbledick[61], V. Coco[47], J.A.B. Coelho[11], J. Cogan[10],
E. Cogneras[9], L. Cojocariu[36], P. Collins[47], T. Colombo[47], A. Contu[26], N. Cooke[52], G. Coombs[58],
S. Coquereau[44], G. Corti[47], C.M. Costa Sobral[55], B. Couturier[47], D.C. Craik[63], J. Crkovská[66],
A. Crocombe[55], M. Cruz Torres[1,z], R. Currie[57], C.L. Da Silva[66], E. Dall'Occo[14], J. Dalseno[45,53],
C. D'Ambrosio[47], A. Danilina[38], P. d'Argent[47], A. Davis[61], O. De Aguiar Francisco[47],
K. De Bruyn[47], S. De Capua[61], M. De Cian[48], J.M. De Miranda[1], L. De Paula[2], M. De Serio[18,d],
P. De Simone[22], J.A. de Vries[76], C.T. Dean[66], W. Dean[81], D. Decamp[8], L. Del Buono[12],
B. Delaney[54], H.-P. Dembinski[14], A. Dendek[34], V. Denysenko[49], D. Derkach[79], O. Deschamps[9],
F. Desse[11], F. Dettori[26,f], B. Dey[7], A. Di Canto[47], P. Di Nezza[22], S. Didenko[78], H. Dijkstra[47],
V. Dobishuk[51], F. Dordei[26], M. Dorigo[28,x], A.C. dos Reis[1], L. Douglas[58], A. Dovbnya[50],
K. Dreimanis[59], M.W. Dudek[33], L. Dufour[47], P. Durante[47], J.M. Durham[66], D. Dutta[61],
M. Dziewiecki[16], A. Dziurda[33], A. Dzyuba[37], S. Easo[56], U. Egede[69], V. Egorychev[38],
S. Eidelman[42,w], S. Eisenhardt[57], S. Ek-In[48], L. Eklund[58], S. Ely[67], A. Ene[36], E. Epple[66],
S. Escher[13], J. Eschle[49], S. Esen[31], T. Evans[47], A. Falabella[19], J. Fan[3], Y. Fan[5], N. Farley[52],
S. Farry[59], D. Fazzini[11], P. Fedin[38], M. Féo[47], P. Fernandez Declara[47], A. Fernandez Prieto[45],
F. Ferrari[19,e], L. Ferreira Lopes[48], F. Ferreira Rodrigues[2], S. Ferreres Sole[31], M. Ferrillo[49],
M. Ferro-Luzzi[47], S. Filippov[40], R.A. Fini[18], M. Fiorini[20,g], M. Firlej[34], K.M. Fischer[62],
C. Fitzpatrick[61], T. Fiutowski[34], F. Fleuret[11,b], M. Fontana[47], F. Fontanelli[23,h], R. Forty[47],
V. Franco Lima[59], M. Franco Sevilla[65], M. Frank[47], C. Frei[47], D.A. Friday[58], J. Fu[25,p],

Q. Fuehring[14], W. Funk[47], E. Gabriel[57], T. Gaintseva[41], A. Gallas Torreira[45], D. Galli[19,e],
S. Gallorini[27], S. Gambetta[57], Y. Gan[3], M. Gandelman[2], P. Gandini[25], Y. Gao[4],
L.M. Garcia Martin[46], J. García Pardiñas[49], B. Garcia Plana[45], F.A. Garcia Rosales[11],
L. Garrido[44], D. Gascon[44], C. Gaspar[47], D. Gerick[16], E. Gersabeck[61], M. Gersabeck[61],
T. Gershon[55], D. Gerstel[10], Ph. Ghez[8], V. Gibson[54], A. Gioventù[45], P. Gironella Gironell[44],
L. Giubega[36], C. Giugliano[20,g], K. Gizdov[57], V.V. Gligorov[12], C. Göbel[70], E. Golobardes[44,l],
D. Golubkov[38], A. Golutvin[60,78], A. Gomes[1,a], P. Gorbounov[38], I.V. Gorelov[39], C. Gotti[24,i],
E. Govorkova[31], J.P. Grabowski[16], R. Graciani Diaz[44], T. Grammatico[12],
L.A. Granado Cardoso[47], E. Graugés[44], E. Graverini[48], G. Graziani[21], A. Grecu[36], R. Greim[31],
P. Griffith[20,g], L. Grillo[61], L. Gruber[47], B.R. Gruberg Cazon[62], C. Gu[3], M. Guarise[20], P.
A. Günther[16], E. Gushchin[40], A. Guth[13], Yu. Guz[43,47], T. Gys[47], T. Hadavizadeh[62], G. Haefeli[48],
C. Haen[47], S.C. Haines[54], P.M. Hamilton[65], Q. Han[7], X. Han[16], T.H. Hancock[62],
S. Hansmann-Menzemer[16], N. Harnew[62], T. Harrison[59], R. Hart[31], C. Hasse[14], M. Hatch[47],
J. He[5], M. Hecker[60], K. Heijhoff[31], K. Heinicke[14], A.M. Hennequin[47], K. Hennessy[59],
L. Henry[25,46], J. Heuel[13], A. Hicheur[68], D. Hill[62], M. Hilton[61], P.H. Hopchev[48], J. Hu[16], J. Hu[71],
W. Hu[7], W. Huang[5], W. Hulsbergen[31], T. Humair[60], R.J. Hunter[55], M. Hushchyn[79],
D. Hutchcroft[59], D. Hynds[31], P. Ibis[14], M. Idzik[34], P. Ilten[52], A. Inglessi[37], K. Ivshin[37],
R. Jacobsson[47], S. Jakobsen[47], E. Jans[31], B.K. Jashal[46], A. Jawahery[65], V. Jevtic[14], F. Jiang[3],
M. John[62], D. Johnson[47], C.R. Jones[54], B. Jost[47], N. Jurik[62], S. Kandybei[50], M. Karacson[47],
J.M. Kariuki[53], N. Kazeev[79], M. Kecke[16], F. Keizer[54,47], M. Kelsey[67], M. Kenzie[55], T. Ketel[32],
B. Khanji[47], A. Kharisova[80], K.E. Kim[67], T. Kirn[13], V.S. Kirsebom[48], S. Klaver[22],
K. Klimaszewski[35], S. Koliiev[51], A. Kondybayeva[78], A. Konoplyannikov[38], P. Kopciewicz[34],
R. Kopecna[16], P. Koppenburg[31], M. Korolev[39], I. Kostiuk[31,51], O. Kot[51], S. Kotriakhova[37],
L. Kravchuk[40], R.D. Krawczyk[47], M. Kreps[55], F. Kress[60], S. Kretzschmar[13], P. Krokovny[42,w],
W. Krupa[34], W. Krzemien[35], W. Kucewicz[33,k], M. Kucharczyk[33], V. Kudryavtsev[42,w],
H.S. Kuindersma[31], G.J. Kunde[66], T. Kvaratskheliya[38], D. Lacarrere[47], G. Lafferty[61], A. Lai[26],
D. Lancierini[49], J.J. Lane[61], G. Lanfranchi[22], C. Langenbruch[13], O. Lantwin[49], T. Latham[55],
F. Lazzari[28,u], R. Le Gac[10], S.H. Lee[81], R. Lefèvre[9], A. Leflat[39,47], O. Leroy[10], T. Lesiak[33],
B. Leverington[16], H. Li[71], L. Li[62], X. Li[66], Y. Li[6], Z. Li[67], X. Liang[67], T. Lin[60], R. Lindner[47],
V. Lisovskyi[14], G. Liu[71], X. Liu[3], D. Loh[55], A. Loi[26], J. Lomba Castro[45], I. Longstaff[58],
J.H. Lopes[2], G. Loustau[49], G.H. Lovell[54], Y. Lu[6], D. Lucchesi[27,n], M. Lucio Martinez[31], Y. Luo[3],
A. Lupato[61], E. Luppi[20,g], O. Lupton[55], A. Lusiani[28,s], X. Lyu[5], S. Maccolini[19,e], F. Machefert[11],
F. Maciuc[36], V. Macko[48], P. Mackowiak[14], S. Maddrell-Mander[53], L.R. Madhan Mohan[53],
O. Maev[37], A. Maevskiy[79], D. Maisuzenko[37], M.W. Majewski[34], S. Malde[62], B. Malecki[47],
A. Malinin[77], T. Maltsev[42,w], H. Malygina[16], G. Manca[26,f], G. Mancinelli[10],
R. Manera Escalero[44], D. Manuzzi[19,e], D. Marangotto[25,p], J. Maratas[9,v], J.F. Marchand[8],
U. Marconi[19], S. Mariani[21,47,21], C. Marin Benito[11], M. Marinangeli[48], P. Marino[48], J. Marks[16],
P.J. Marshall[59], G. Martellotti[30], L. Martinazzoli[47], M. Martinelli[24,i], D. Martinez Santos[45],
F. Martinez Vidal[46], A. Massafferri[1], M. Materok[13], R. Matev[47], A. Mathad[49], Z. Mathe[47],
V. Matiunin[38], C. Matteuzzi[24], K.R. Mattioli[81], A. Mauri[49], E. Maurice[11,b], M. McCann[60],
L. Mcconnell[17], A. McNab[61], R. McNulty[17], J.V. Mead[59], B. Meadows[64], C. Meaux[10],
G. Meier[14], N. Meinert[74], D. Melnychuk[35], S. Meloni[24,i], M. Merk[31], A. Merli[25],
L. Meyer Garcia[2], M. Mikhasenko[47], D.A. Milanes[73], E. Millard[55], M.-N. Minard[8], O. Mineev[38],
L. Minzoni[20,g], S.E. Mitchell[57], B. Mitreska[61], D.S. Mitzel[47], A. Mödden[14], A. Mogini[12],
R.D. Moise[60], T. Mombächer[14], I.A. Monroy[73], S. Monteil[9], M. Morandin[27], G. Morello[22],
M.J. Morello[28,s], J. Moron[34], A.B. Morris[10], A.G. Morris[55], R. Mountain[67], H. Mu[3],
F. Muheim[57], M. Mukherjee[7], M. Mulder[47], D. Müller[47], K. Müller[49], C.H. Murphy[62],
D. Murray[61], P. Muzzetto[26], P. Naik[53], T. Nakada[48], R. Nandakumar[56], T. Nanut[48], I. Nasteva[2],

M. Needham[57], I. Neri[20,g], N. Neri[25,p], S. Neubert[16], N. Neufeld[47], R. Newcombe[60],
T.D. Nguyen[48], C. Nguyen-Mau[48,m], E.M. Niel[11], S. Nieswand[13], N. Nikitin[39], N.S. Nolte[47],
C. Nunez[81], A. Oblakowska-Mucha[34], V. Obraztsov[43], S. Ogilvy[58], D.P. O'Hanlon[53],
R. Oldeman[26,f], C.J.G. Onderwater[75], J. D. Osborn[81], A. Ossowska[33], J.M. Otalora Goicochea[2],
T. Ovsiannikova[38], P. Owen[49], A. Oyanguren[46], P.R. Pais[48], T. Pajero[28,47,28,s], A. Palano[18],
M. Palutan[22], G. Panshin[80], A. Papanestis[56], M. Pappagallo[57], L.L. Pappalardo[20,g],
C. Pappenheimer[64], W. Parker[65], C. Parkes[61], G. Passaleva[21,47], A. Pastore[18], M. Patel[60],
C. Patrignani[19,e], A. Pearce[47], A. Pellegrino[31], M. Pepe Altarelli[47], S. Perazzini[19], D. Pereima[38],
P. Perret[9], K. Petridis[53], A. Petrolini[23,h], A. Petrov[77], S. Petrucci[57], M. Petruzzo[25,p],
B. Pietrzyk[8], G. Pietrzyk[48], M. Pili[62], D. Pinci[30], J. Pinzino[47], F. Pisani[19], A. Piucci[16],
V. Placinta[36], S. Playfer[57], J. Plews[52], M. Plo Casasus[45], F. Polci[12], M. Poli Lener[22],
M. Poliakova[67], A. Poluektov[10], N. Polukhina[78,c], I. Polyakov[67], E. Polycarpo[2], G.J. Pomery[53],
S. Ponce[47], A. Popov[43], D. Popov[52], S. Poslavskii[43], K. Prasanth[33], L. Promberger[47],
C. Prouve[45], V. Pugatch[51], A. Puig Navarro[49], H. Pullen[62], G. Punzi[28,o], W. Qian[5], J. Qin[5],
R. Quagliani[12], B. Quintana[8], N.V. Raab[17], R.I. Rabadan Trejo[10], B. Rachwal[34],
J.H. Rademacker[53], M. Rama[28], M. Ramos Pernas[45], M.S. Rangel[2], F. Ratnikov[41,79], G. Raven[32],
M. Reboud[8], F. Redi[48], F. Reiss[12], C. Remon Alepuz[46], Z. Ren[3], V. Renaudin[62], S. Ricciardi[56],
D.S. Richards[56], S. Richards[53], K. Rinnert[59], P. Robbe[11], A. Robert[12], A.B. Rodrigues[48],
E. Rodrigues[59], J.A. Rodriguez Lopez[73], M. Roehrken[47], A. Rollings[62], V. Romanovskiy[43],
M. Romero Lamas[45], A. Romero Vidal[45], J.D. Roth[81], M. Rotondo[22], M.S. Rudolph[67], T. Ruf[47],
J. Ruiz Vidal[46], A. Ryzhikov[79], J. Ryzka[34], J.J. Saborido Silva[45], N. Sagidova[37], N. Sahoo[55],
B. Saitta[26,f], C. Sanchez Gras[31], C. Sanchez Mayordomo[46], R. Santacesaria[30],
C. Santamarina Rios[45], M. Santimaria[22], E. Santovetti[29,j], G. Sarpis[61], M. Sarpis[16], A. Sarti[30],
C. Satriano[30,r], A. Satta[29], M. Saur[5], D. Savrina[38,39], L.G. Scantlebury Smead[62], S. Schael[13],
M. Schellenberg[14], M. Schiller[58], H. Schindler[47], M. Schmelling[15], T. Schmelzer[14], B. Schmidt[47],
O. Schneider[48], A. Schopper[47], H.F. Schreiner[64], M. Schubiger[31], S. Schulte[48], M.H. Schune[11],
R. Schwemmer[47], B. Sciascia[22], A. Sciubba[22], S. Sellam[68], A. Semennikov[38], A. Sergi[52,47],
N. Serra[49], J. Serrano[10], L. Sestini[27], A. Seuthe[14], P. Seyfert[47], D.M. Shangase[81], M. Shapkin[43],
L. Shchutska[48], T. Shears[59], L. Shekhtman[42,w], V. Shevchenko[77], E. Shmanin[78], J.D. Shupperd[67],
B.G. Siddi[20], R. Silva Coutinho[49], L. Silva de Oliveira[2], G. Simi[27,n], S. Simone[18,d], I. Skiba[20,g],
N. Skidmore[16], T. Skwarnicki[67], M.W. Slater[52], J.G. Smeaton[54], A. Smetkina[38], E. Smith[13],
I.T. Smith[57], M. Smith[60], A. Snoch[31], M. Soares[19], L. Soares Lavra[9], M.D. Sokoloff[64],
F.J.P. Soler[58], B. Souza De Paula[2], B. Spaan[14], E. Spadaro Norella[25,p], P. Spradlin[58], F. Stagni[47],
M. Stahl[64], S. Stahl[47], P. Stefko[48], O. Steinkamp[49,78], S. Stemmle[16], O. Stenyakin[43],
M. Stepanova[37], H. Stevens[14], S. Stone[67], S. Stracka[28], M.E. Stramaglia[48], M. Straticiuc[36],
S. Strokov[80], J. Sun[26], L. Sun[72], Y. Sun[65], P. Svihra[61], K. Swientek[34], A. Szabelski[35],
T. Szumlak[34], M. Szymanski[47], S. Taneja[61], Z. Tang[3], T. Tekampe[14], F. Teubert[47], E. Thomas[47],
K.A. Thomson[59], M.J. Tilley[60], V. Tisserand[9], S. T'Jampens[8], M. Tobin[6], S. Tolk[47],
L. Tomassetti[20,g], D. Torres Machado[1], D.Y. Tou[12], E. Tournefier[8], M. Traill[58], M.T. Tran[48],
E. Trifonova[78], C. Trippl[48], A. Tsaregorodtsev[10], G. Tuci[28,o], A. Tully[48], N. Tuning[31],
A. Ukleja[35], A. Usachov[31], A. Ustyuzhanin[41,79], U. Uwer[16], A. Vagner[80], V. Vagnoni[19],
A. Valassi[47], G. Valenti[19], M. van Beuzekom[31], H. Van Hecke[66], E. van Herwijnen[47],
C.B. Van Hulse[17], M. van Veghel[75], R. Vazquez Gomez[44], P. Vazquez Regueiro[45],
C. Vázquez Sierra[31], S. Vecchi[20], J.J. Velthuis[53], M. Veltri[21,q], A. Venkateswaran[67],
M. Veronesi[31], M. Vesterinen[55], J.V. Viana Barbosa[47], D. Vieira[64], M. Vieites Diaz[48],
H. Viemann[74], X. Vilasis-Cardona[44,l], G. Vitali[28], A. Vitkovskiy[31], A. Vollhardt[49],
D. Vom Bruch[12], A. Vorobyev[37], V. Vorobyev[42,w], N. Voropaev[37], R. Waldi[74], J. Walsh[28],
J. Wang[3], J. Wang[72], J. Wang[6], M. Wang[3], Y. Wang[7], Z. Wang[49], D.R. Ward[54], H.M. Wark[59],

N.K. Watson[52], D. Websdale[60], A. Weiden[49], C. Weisser[63], B.D.C. Westhenry[53], D.J. White[61], M. Whitehead[53], D. Wiedner[14], G. Wilkinson[62], M. Wilkinson[67], I. Williams[54], M. Williams[63], M.R.J. Williams[61], T. Williams[52], F.F. Wilson[56], W. Wislicki[35], M. Witek[33], L. Witola[16], G. Wormser[11], S.A. Wotton[54], H. Wu[67], K. Wyllie[47], Z. Xiang[5], D. Xiao[7], Y. Xie[7], H. Xing[71], A. Xu[4], J. Xu[5], L. Xu[3], M. Xu[7], Q. Xu[5], Z. Xu[4], Z. Yang[3], Z. Yang[65], Y. Yao[67], L.E. Yeomans[59], H. Yin[7], J. Yu[7], X. Yuan[67], O. Yushchenko[43], K.A. Zarebski[52], M. Zavertyaev[15,c], M. Zdybal[33], M. Zeng[3], D. Zhang[7], L. Zhang[3], S. Zhang[4], W.C. Zhang[3,y], Y. Zhang[47], A. Zhelezov[16], Y. Zheng[5], X. Zhou[5], Y. Zhou[5], X. Zhu[3], V. Zhukov[13,39], J.B. Zonneveld[57], S. Zucchelli[19,e]

[1] Centro Brasileiro de Pesquisas Físicas (CBPF), Rio de Janeiro, Brazil
[2] Universidade Federal do Rio de Janeiro (UFRJ), Rio de Janeiro, Brazil
[3] Center for High Energy Physics, Tsinghua University, Beijing, China
[4] School of Physics State Key Laboratory of Nuclear Physics and Technology, Peking University, Beijing, China
[5] University of Chinese Academy of Sciences, Beijing, China
[6] Institute Of High Energy Physics (IHEP), Beijing, China
[7] Institute of Particle Physics, Central China Normal University, Wuhan, Hubei, China
[8] Univ. Grenoble Alpes, Univ. Savoie Mont Blanc, CNRS, IN2P3-LAPP, Annecy, France
[9] Université Clermont Auvergne, CNRS/IN2P3, LPC, Clermont-Ferrand, France
[10] Aix Marseille Univ, CNRS/IN2P3, CPPM, Marseille, France
[11] Université Paris-Saclay, CNRS/IN2P3, IJCLab, Orsay, France
[12] LPNHE, Sorbonne Université, Paris Diderot Paris Cité, CNRS/IN2P3, Paris, France
[13] I. Physikalisches Institut, RWTH Aachen University, Aachen, Germany
[14] Fakultät Physik, Technische Universität Dortmund, Dortmund, Germany
[15] Max-Planck-Institut für Kernphysik (MPIK), Heidelberg, Germany
[16] Physikalisches Institut, Ruprecht-Karls-Universität Heidelberg, Heidelberg, Germany
[17] School of Physics, University College Dublin, Dublin, Ireland
[18] INFN Sezione di Bari, Bari, Italy
[19] INFN Sezione di Bologna, Bologna, Italy
[20] INFN Sezione di Ferrara, Ferrara, Italy
[21] INFN Sezione di Firenze, Firenze, Italy
[22] INFN Laboratori Nazionali di Frascati, Frascati, Italy
[23] INFN Sezione di Genova, Genova, Italy
[24] INFN Sezione di Milano-Bicocca, Milano, Italy
[25] INFN Sezione di Milano, Milano, Italy
[26] INFN Sezione di Cagliari, Monserrato, Italy
[27] INFN Sezione di Padova, Padova, Italy
[28] INFN Sezione di Pisa, Pisa, Italy
[29] INFN Sezione di Roma Tor Vergata, Roma, Italy
[30] INFN Sezione di Roma La Sapienza, Roma, Italy
[31] Nikhef National Institute for Subatomic Physics, Amsterdam, Netherlands
[32] Nikhef National Institute for Subatomic Physics and VU University Amsterdam, Amsterdam, Netherlands
[33] Henryk Niewodniczanski Institute of Nuclear Physics Polish Academy of Sciences, Kraków, Poland
[34] AGH — University of Science and Technology, Faculty of Physics and Applied Computer Science, Kraków, Poland
[35] National Center for Nuclear Research (NCBJ), Warsaw, Poland
[36] Horia Hulubei National Institute of Physics and Nuclear Engineering, Bucharest-Magurele, Romania
[37] Petersburg Nuclear Physics Institute NRC Kurchatov Institute (PNPI NRC KI), Gatchina, Russia
[38] Institute of Theoretical and Experimental Physics NRC Kurchatov Institute (ITEP NRC KI), Moscow, Russia, Moscow, Russia

39 *Institute of Nuclear Physics, Moscow State University (SINP MSU), Moscow, Russia*

40 *Institute for Nuclear Research of the Russian Academy of Sciences (INR RAS), Moscow, Russia*

41 *Yandex School of Data Analysis, Moscow, Russia*

42 *Budker Institute of Nuclear Physics (SB RAS), Novosibirsk, Russia*

43 *Institute for High Energy Physics NRC Kurchatov Institute (IHEP NRC KI), Protvino, Russia, Protvino, Russia*

44 *ICCUB, Universitat de Barcelona, Barcelona, Spain*

45 *Instituto Galego de Física de Altas Enerxías (IGFAE), Universidade de Santiago de Compostela, Santiago de Compostela, Spain*

46 *Instituto de Fisica Corpuscular, Centro Mixto Universidad de Valencia — CSIC, Valencia, Spain*

47 *European Organization for Nuclear Research (CERN), Geneva, Switzerland*

48 *Institute of Physics, Ecole Polytechnique Fédérale de Lausanne (EPFL), Lausanne, Switzerland*

49 *Physik-Institut, Universität Zürich, Zürich, Switzerland*

50 *NSC Kharkiv Institute of Physics and Technology (NSC KIPT), Kharkiv, Ukraine*

51 *Institute for Nuclear Research of the National Academy of Sciences (KINR), Kyiv, Ukraine*

52 *University of Birmingham, Birmingham, United Kingdom*

53 *H.H. Wills Physics Laboratory, University of Bristol, Bristol, United Kingdom*

54 *Cavendish Laboratory, University of Cambridge, Cambridge, United Kingdom*

55 *Department of Physics, University of Warwick, Coventry, United Kingdom*

56 *STFC Rutherford Appleton Laboratory, Didcot, United Kingdom*

57 *School of Physics and Astronomy, University of Edinburgh, Edinburgh, United Kingdom*

58 *School of Physics and Astronomy, University of Glasgow, Glasgow, United Kingdom*

59 *Oliver Lodge Laboratory, University of Liverpool, Liverpool, United Kingdom*

60 *Imperial College London, London, United Kingdom*

61 *Department of Physics and Astronomy, University of Manchester, Manchester, United Kingdom*

62 *Department of Physics, University of Oxford, Oxford, United Kingdom*

63 *Massachusetts Institute of Technology, Cambridge, MA, United States*

64 *University of Cincinnati, Cincinnati, OH, United States*

65 *University of Maryland, College Park, MD, United States*

66 *Los Alamos National Laboratory (LANL), Los Alamos, United States*

67 *Syracuse University, Syracuse, NY, United States*

68 *Laboratory of Mathematical and Subatomic Physics, Constantine, Algeria, associated to [2]*

69 *School of Physics and Astronomy, Monash University, Melbourne, Australia, associated to [55]*

70 *Pontifícia Universidade Católica do Rio de Janeiro (PUC-Rio), Rio de Janeiro, Brazil, associated to [2]*

71 *Guangdong Provencial Key Laboratory of Nuclear Science, Institute of Quantum Matter, South China Normal University, Guangzhou, China, associated to [3]*

72 *School of Physics and Technology, Wuhan University, Wuhan, China, associated to [3]*

73 *Departamento de Fisica, Universidad Nacional de Colombia, Bogota, Colombia, associated to [12]*

74 *Institut für Physik, Universität Rostock, Rostock, Germany, associated to [16]*

75 *Van Swinderen Institute, University of Groningen, Groningen, Netherlands, associated to [31]*

76 *Universiteit Maastricht, Maastricht, Netherlands, associated to [31]*

77 *National Research Centre Kurchatov Institute, Moscow, Russia, associated to [38]*

78 *National University of Science and Technology "MISIS", Moscow, Russia, associated to [38]*

79 *National Research University Higher School of Economics, Moscow, Russia, associated to [41]*

80 *National Research Tomsk Polytechnic University, Tomsk, Russia, associated to [38]*

81 *University of Michigan, Ann Arbor, United States, associated to [67]*

[a] *Universidade Federal do Triângulo Mineiro (UFTM), Uberaba-MG, Brazil*

[b] *Laboratoire Leprince-Ringuet, Palaiseau, France*

[c] *P.N. Lebedev Physical Institute, Russian Academy of Science (LPI RAS), Moscow, Russia*

[d] *Università di Bari, Bari, Italy*

[e] Università di Bologna, Bologna, Italy

[f] Università di Cagliari, Cagliari, Italy

[g] Università di Ferrara, Ferrara, Italy

[h] Università di Genova, Genova, Italy

[i] Università di Milano Bicocca, Milano, Italy

[j] Università di Roma Tor Vergata, Roma, Italy

[k] AGH — University of Science and Technology, Faculty of Computer Science, Electronics and Telecommunications, Kraków, Poland

[l] DS4DS, La Salle, Universitat Ramon Llull, Barcelona, Spain

[m] Hanoi University of Science, Hanoi, Vietnam

[n] Università di Padova, Padova, Italy

[o] Università di Pisa, Pisa, Italy

[p] Università degli Studi di Milano, Milano, Italy

[q] Università di Urbino, Urbino, Italy

[r] Università della Basilicata, Potenza, Italy

[s] Scuola Normale Superiore, Pisa, Italy

[t] Università di Modena e Reggio Emilia, Modena, Italy

[u] Università di Siena, Siena, Italy

[v] MSU — Iligan Institute of Technology (MSU-IIT), Iligan, Philippines

[w] Novosibirsk State University, Novosibirsk, Russia

[x] INFN Sezione di Trieste, Trieste, Italy

[y] School of Physics and Information Technology, Shaanxi Normal University (SNNU), Xi'an, China

[z] Universidad Nacional Autonoma de Honduras, Tegucigalpa, Honduras